KSCE Journal of Civil Engineering (2016) 20(6):2297-2307
DOI 10.1007/s12205-015-0221-7

Geotechnical Engineering
pISSN 1226-7988, eISSN 1976-3808
www.springer.com/12205

Coefficient of Restitution and Kinetic Energy Loss of Rockfall Impacts

Li-ping Li*, Shang-qu Sun, Shu-cai Li***, Qian-qing Zhang****, Cong Hu*****, and Shao-shuai Shi******

Received March 14, 2015/Revised July 27, 2015/Accepted September 10, 2015/Published Online November 13, 2015

Abstract

This paper presents the results of the coefficient of restitution and the kinetic energy loss rate obtained by lab experiment, two parameters that are crucial for rockfall impact. However, various definitions of coefficient of restitution exist and the most appropriate one is still not formed and obtained. In addition, the energy variation during the rockfall impacts has important significance in practical design. In this research, two kind shapes of blocks including plate and strip were adopted in the laboratory testing and the block material was tested before, indicating that the material has sufficient strength to prevent shattering during the impact. Furthermore, an apparatus specifically built for this study was established including a base, a slope and a releasing device. The falling testing was performed using plate and strip block while the falling height as well as the slope angle and releasing height were altered during the tests in order to estimate the effect of each parameter on the coefficients of restitution and energy loss rate. It was observed that collision reflection angle is less than impact angle for all, suggesting energy loss in collision. Impact angle decreases with increasing slope angle while there was no obvious effect of releasing height and releasing angle on impact angle. The relevant coefficient of restitution was found to decrease with impact angle, and the kinetic energy loss rate increased. Finally, the kinetic energy before and after the impact was found to significantly affect the COR and energy loss rate and the results can provide basis for mitigation measures.

Keywords: *rockfall, coefficient of restitution, kinetic energy, lab experiment, impact angle*

1. Introduction

Rockfall is a common geological hazard in the world's mountainous regions. On account of its sudden and high frequency, a serious threat to the surrounding human and infrastructure arises (Pantelidis, 2009; Pantelidis, 2010). Therefore, the research on rockfall is of great significance for its forecast and mitigation. To illustrate the rockfall problem, Fig. 1 shows a rockfall event which occurred in Sichuan province on July 25, 2009. A rock of more than 50 m^3, 130 ton fell on the Di guan bridge, causing 6 death and 12 people injured and Ying wen road cut off for 5 days.

The trajectory of a block is regarded as a combination of four basic block movement types: free falling, bouncing, rolling and sliding (Descoeudres and Zimmermann, 1987). To reduce rocakfall havard, mitigation measures including rock bolts, intercepting ditches, SNS flexible nets have been extensively used (Agliardi and Crosta, 2003). The design of these rockfall mitigations is based on the trajectory of rockfall and the level of kinetic energy at the location where the mitigation devices are necessary to be installed However, the observation of the process of collision should be improved because of the randomness of the impacting occurrence and even the density of the soil slope can affect the result (Guzzetti *et al*., 2002). As to the trajectories of the rolling stones, the bouncing height and the kinetic energy loss can be usually achieved by using numerical simulation software such as RocFall (Stevens 1998) or CRSP (Pfeiffer and Bowen, 1989). The most crucial input parameter is the Coefficient of Restitution (COR), which plays a key role in numerical simulation and can be determined by laboratory, field test and back analysis (Asteriou *et al*., 2012).

Many rock fall field tests have been conducted by several scholars to obtain the COR. Huang (2007) carried on a series of orthogonal experiments, and analyzed the effects of angle and

*Associate Professor, Research Center of Geotechnical and Structural Engineering, Shandong University, Jinan, China, Nanjing Hydraulic Research Institute (E-mail: yuliyangfan@163.com)
**Ph.D Student, Research Center of Geotechnical and Structural Engineering, Shandong University, Jinan, China (Corresponding Author, E-mail: sunshangqu@163.com)
***Professor, Research Center of Geotechnical and Structural Engineering, Shandong University, Jinan, China (E-mail: lishucai@sdu.edu.cn)
****Ph.D, Research Center of Geotechnical and Structural Engineering, Shandong University, Jinan, China (E-mail: zjuzqq@163.com)
*****Ph.D Student, Laboratoire de Mecanique de Lille (LML), Ecole Centrale de Lille, BP48, F-59651Villeneuve d'Ascq Cedex, France (E-mail: hucongsdu@sina.com)
******Ph.D, Research Center of Geotechnical and Structural Engineering, Shandong University, Jinan, China (E-mail: sss_sdu@163.com)

(a) (b)

Fig. 1. A rocakfall Disaster Occurred in Yingwen Road of China: (a) The Damaged Bridge, (b) The Falling Rock

length of the slope on the trajectories of the rolling stones. Field test on the coefficient of restitution was carried out by P.Asreriou, and the result was found to verify the reliability of lab experiment and be effective on rockfall mitigation (Asteriou *et al*., 2012). In addition to field test, laboratory tests have been conducted to study the coefficient of restitution of rockfall impacts. Chau (2002) used spherical boulders made of dental gypsum to simulate falling rocks and studied the relationship between the normal and tangential coefficient of restitution and the slope angle. A simple theoretical prediction model was proposed to determine the variation of rotational energy versus slope angle. Olivier Buzzi (2012) studied the cases that the coefficient of restitution is greater than 1 and the rotational energy, the shape of block and glancing collision were considered. At present, lack of thorough study on the coefficient of restitution is still a major challenge for which no fully satisfactory solution has existed up until now.

The present study is undertaken to focus on the changing law of coefficient of restitution and energy loss rate with the releasing conditions including the slope angle, releasing height, block shape and impact angle. In addition, the kinetic energy loss during the collision is another crucial parameter which determines the strength of the protective measures. Therefore, the kinetic energy before and after the impact was studied and found to significantly affect the COR and energy loss rate

2. Coefficient of Restitution and Kinetic Energy Loss Rate

The coefficient of restitution is commonly defined as the ratio of the resultant velocities before and after an impact of two colliding entities, which has been adopted by many authors (Spang and Sonser, 1995; Paronuzzi, 1989; Spang and Rautenstrauch, 1988; Japan-Road-Association, 1983; Azzoni and De Freitas, 1995). Theoretically, COR equals one in the case of perfect elastic collision without rotational velocity considered before and after rebound, and zero versus a perfectly plastic collision without bouncing. However, the collision is always accompanied with energy loss, which determines COR is normally between 0 and 1 (Asteriou *et al*., 2012).

The following definition of COR is based on the lumped-mass impact theory and probably had its origins in the time of Newton when particle collision dynamics was considered, known as kinematic coefficient of restitution:

$$R_v = \frac{V_r}{V_i} \tag{1}$$

where V_r and V_i are the rebounding velocity and incoming velocity of rockfall, respectively.

To further study the variation of kinetic energy during the rockfall impacting, the concept of the loss rate of kinetic energy is adopted in the present paper and it can be expressed by the following form:

$$\gamma = \frac{\frac{1}{2}mV_i^2 - \frac{1}{2}mV_r^2}{\frac{1}{2}mV_i^2} = \frac{V_i^2 - V_r^2}{V_i^2} \tag{2}$$

where m is the mass of the block. The definition has been used and adopted by Chau *et al.* (1999), Azzoni *et al.* (1995), and Bozzolo and Pamini (1986).

It can be concluded from Eqs. (1) and (2) that the rebounding velocity and incoming velocity of rockfall are key parameters to determine the COR. In the present paper, the method proposed by K T Chau (2002) is adopted to calculate the velocity of rockfall. The position at any time was recorded by digital camera and the slope angle was determined by protractor. Once these parameters were obtained, the incoming and rebounding velocity can be calculateed respectively with kinematics equation.

Figure 2 shows the position and time and the slope angle α. The normal and tangential component of the incoming and rebounding velocity can be calculated by:

$$V_{in} = \left(\frac{H}{T_1} + \frac{1}{2}gT_1\right)\cos\alpha - \frac{s}{T_1}\sin\alpha \tag{3}$$

$$V_{it} = \left(\frac{H}{T_i} + \frac{1}{2}gT_1\right)\sin\alpha + \frac{s}{T_1}\cos\alpha \tag{4}$$

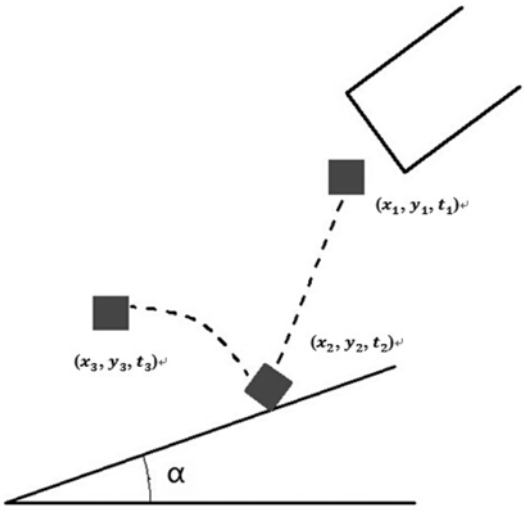

Fig. 2. Recorded Position and Time of Rockfall

$$V_{rn} = \left(\frac{h}{T_2} - \frac{1}{2}gT_2\right)\cos\alpha - \frac{L}{T_2}\sin\alpha \quad (5)$$

$$V_{rt} = \left(\frac{h}{T_2} - \frac{1}{2}gT_2\right)\sin\alpha + \frac{L}{T_2}\cos\alpha \quad (6)$$

where $H = y_1 - y_2$, $h = y_2 - y_3$, $s = x_1 - x_2$, $L = x_2 - x_3$, $T_1 = t_2 - t_1$, $T_2 = t_3 - t_2$ and g is the acceleration of gravity and can be used 9.81 m/s^2.

3. Experimental Studies

3.1 Testing Materials

In the laboratory experiment, falling rock stones were simulated by using mould gypsum of quick setting and strengthening. In the present study, the moisture content of specimens is adopted in the range 30% to 50% when the plaster is made (Chau *et al*., 2002). To further study the properties of this material, standard specimens with a moisture content of 40% were tested by using WDW-100 pressure testing machine (see Fig. 3) to capture the uniaxial compressive strength. The testing results show that the average value of uniaxial compressive strength is 13.37 kN, indicating that the present mould gypsum material has sufficient strength to prevent shattering during the collision.

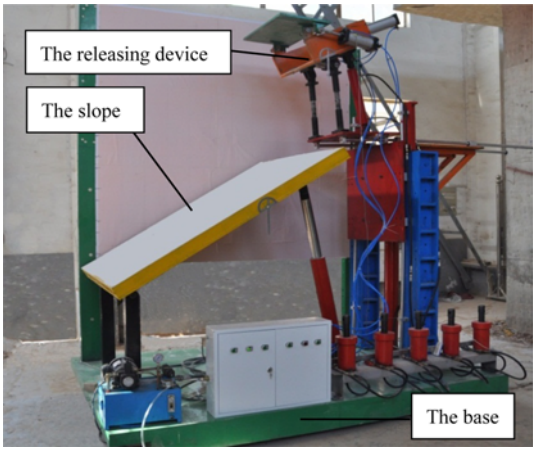

Fig. 4. A Model of the Rockfall Testing System

3.2. Experimental Apparatus

To better study the characteristics of rockfall impacts, an apparatus specifically built for this study was established including a base, a slope and a releasing device (see Fig. 4). The base was made of steel channels and connected by high-strength bolts to keep the stability of structure. In addition, the length of base can be adjusted conveniently according to the testing requirements. The slope was a steel box filled with mold gypsum and connected to the base by using mechanical bearing and steel channels. The releasing device consists of a steel box blocks shot out from and two sliders each controlling the horizontal and vertical direction respectively to make the block in the right position. The lifting jack specifically designed for the testing can

(a) (b)

Fig. 3. Standard Specimens and Testing Machine used in the Present Test: (a) Standard Specimens with a Moisture Content of 40% (b) WDW-100 Pressure Testing machine

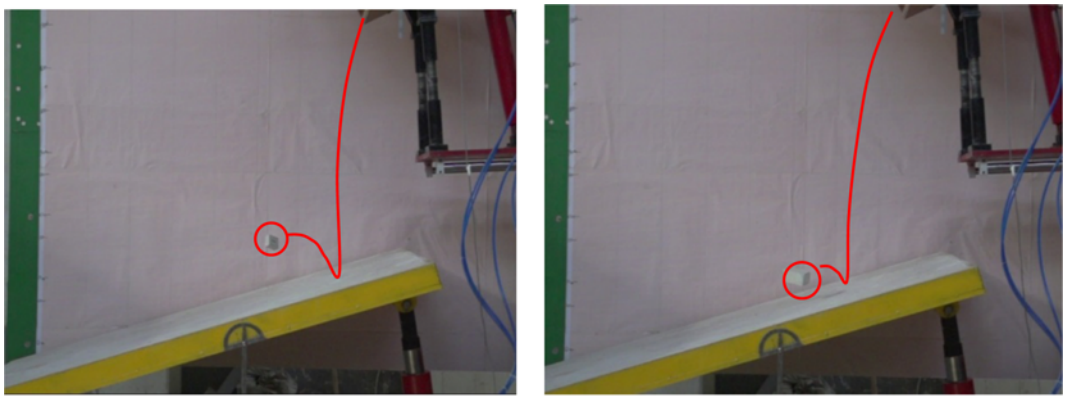

(a) (b)

Fig. 5. Position of Rockfall Collision: (a) for the Plate Block, (b) for the Strip Block

regulate the slope angle from 0° to 30° to fulfill the experimental scheme. Finally, three independent oil pumps were used in the present study, one was to control the slope angle and the other two were to control the position of falling block through the lifting jacks and steel sliders individually.

3.3 Experimental Procedure

In order to capture the trajectories of falling blocks accurately, a high-speed digital camera with a capable of 240 frames per second was used. The video recorded can be replayed frame-by-frame in the computer system to obtain the position corresponding to the time accurately. A reference coordinate system (see Fig. 5) was adopted as the orientation of falling blocks and the axis of the camera was installed perpendicular to the reference grid. Based on the reference coordinate system and the screenshot at some particular moment, the position with the time can be obtained, and then the magnitudes of the rebounding and incoming velocities can be easily calculated by using from Eqs. (3) to (6). The typical trajectories of falling blocks are shown in Fig. 5 and the highest positions of blocks are marked by red circle.

3.4 Experimental Program

The single spherical blocks were used in laboratory test, and the falling blocks used in this study were plate and strip block two forms (see Fig. 6) made of mould gypsum with a moisture content of 40%. Following the suggestion of Ninth International Congress on Rock Mechanics in Paris (Chau *et al*., 1999), relevant preliminary analysis was conducted to investigate the effect of block shape. Two series for 54 testing cases were carried out, the details of which are given in Table 1 and each case was tested with three blocks to account for the randomness of the collision. In the present study, only average experimental results were presented for further analysis. For each series, the angle of slope was adopted as 15°, 20° and 30°, respectively. The releasing angle was taken as 24°, 35° and 50°, respectively. The releasing height was adopted as 60 cm, 75 cm and 100 cm, respectively.

Fig. 6. Plate Block and Strip Block used in the Present Test

Table 1. Detail of Experimental Program

Series	1	2
Block shape	Plate	Strip
Releasing height (cm)	60, 75, 100	60, 75, 100
Slope angle (°)	15, 20, 30	15, 20, 30
Releasing angle (°)	24, 35, 50	24, 35, 50

4. Experimental Results and Discussion

4.1 Effect of Releasing Height and Block Shape

To study the impact of multiple factors, the testing results are displayed by nephogram, the left axis of which is releasing angle and the axis below was slope angle. The coefficient of restitution ranges from 0 to 1 without considering the rotational energy and the experimental error and the changing colors shown in nephogram represent the values of COR. Fig. 7 shows that for the plate block, the largest, the second largest and the smallest COR are observed in the specimen with 60 cm height, 75 cm height, and 100 cm height, respectively. For the plate blocks with 60 cm height, the COR increases from the center to periphery and the maximum value of the COR appears in the slope angle of 22°, rolling angle of 25°. For the plate with 75 cm height, the maximum value of the COR appears in the slope angle of 30°,

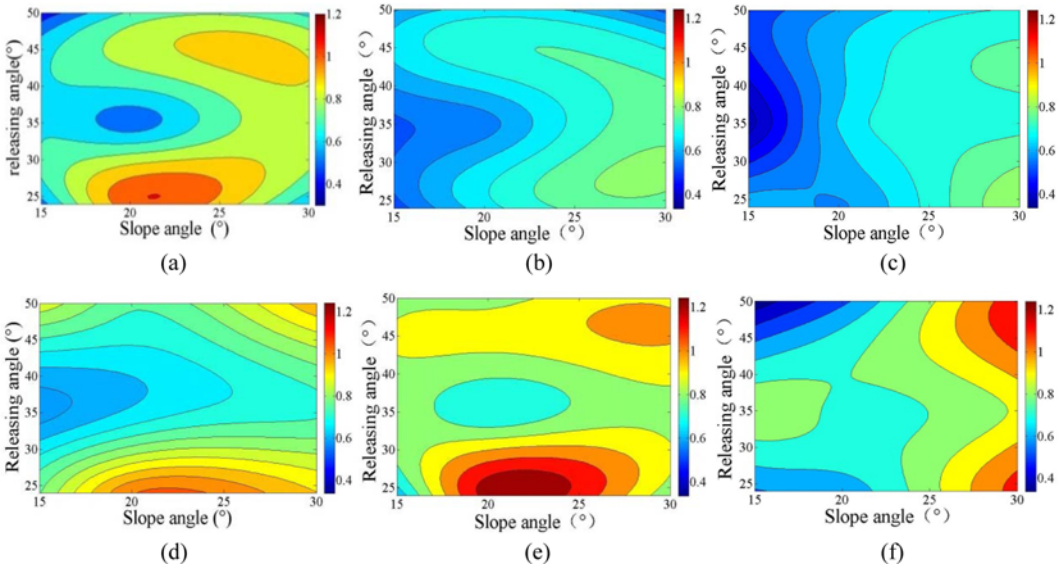

Fig. 7. Effect of Releasing Height and Block Shape on the COR: (a) Plate with Height 60 cm (b) Plate with Height 75 cm, (c) Plate with Height 100 cm, (d) Strip with Height 60 cm, (e) Strip with Height 75 cm, (f) Strip with Height 100 cm

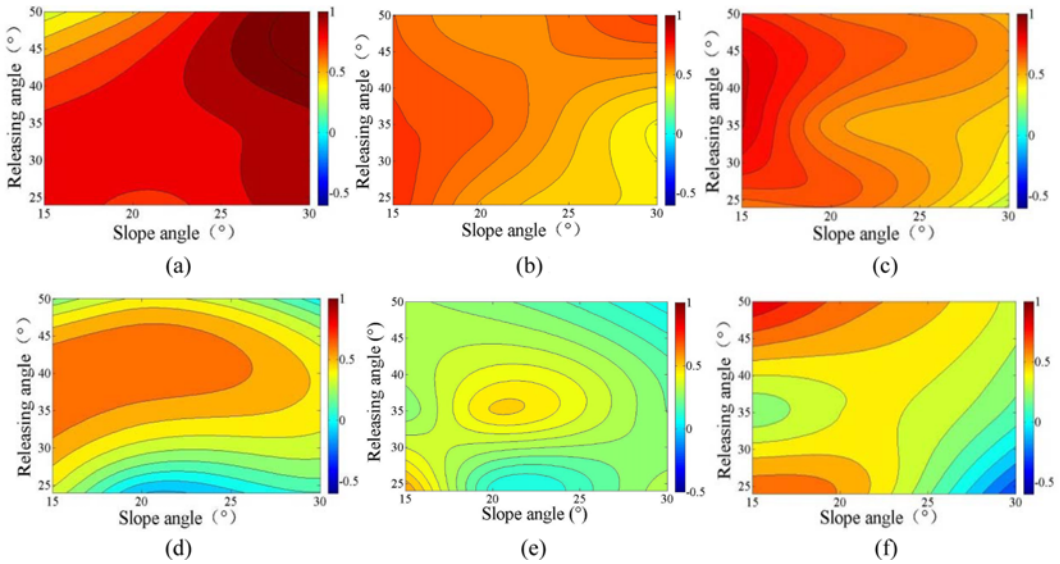

Fig. 8. Effect of Releasing Height and Block Shape on the Kinetic Energy Loss Rate: (a) Plate with Height 60 cm, (b) Plate with Height 75 cm, (c) Plate with Height 100 cm, (d) Strip with Height 60 cm, (e) Strip with Height 75 cm, (f) Strip with Height 100 cm

rolling angle of 28°. For the plate with 100 cm height, the maximum value of the COR appears in the slope angle of 30°, rolling angle of 24°, from where the COR decreases to periphery.

For the same releasing height, COR of the strip and plate blocks were compared and the results showed that COR values of the strip block are larger than that of the plate overall. For the specimens with 75 cm height, the maximum value of the COR appears in the slope angle of 22°, rolling angle of 25° and the values of COR for 60 cm and 100 cm height are rather close.

The effect on kinetic energy loss rate under different operating modes is shown in the same expression way of nephogram, the details of which are presented in Fig. 8. For the plate block, the kinetic energy loss rate in 60 cm height is larger with the maximum values appearing near slope angle 30°and releasing angle 45° rather than 75 cm and 100 cm height. For the strip block, the minimum value of kinetic energy loss rate is obtained in 75 cm height, near slope angle 22° and releasing angle 25° increasing to the periphery. Nevertheless, the rate values in 60 cm and 100 cm height are greater than 75 cm height, suggesting that there is more kinetic energy loss.

4.2 Effect of Slope Angle and Block Shape

Figure 9 plots the COR of plate and strip blocks versus the slope angle α defined in Fig. 2. For the same shape of blocks, by comparing the color from slope angle 15° to 30°, the coefficient of restitution showed apparent increasing trend with the slope

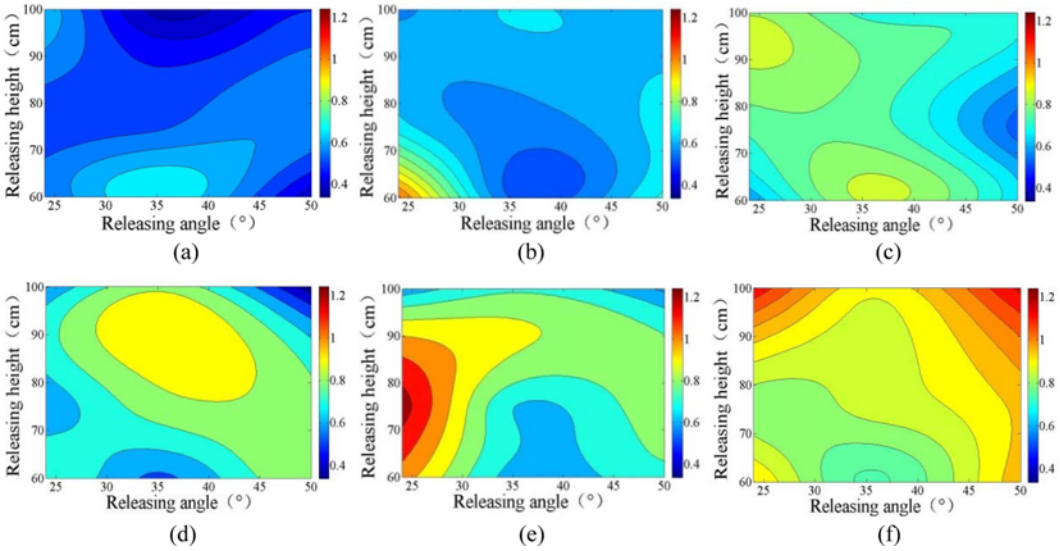

Fig. 9. Effect of Slope Angle and Block Shape on the COR: (a) Plate with Slope Angle 15°, (b) Plate with Slope Angle 20°, (c) Plate with Slope Angle 30°, (d) Strip with Slope Angle 15° (e) Strip with Slope Angle 20°, (f) Strip with Slope Angle 30°

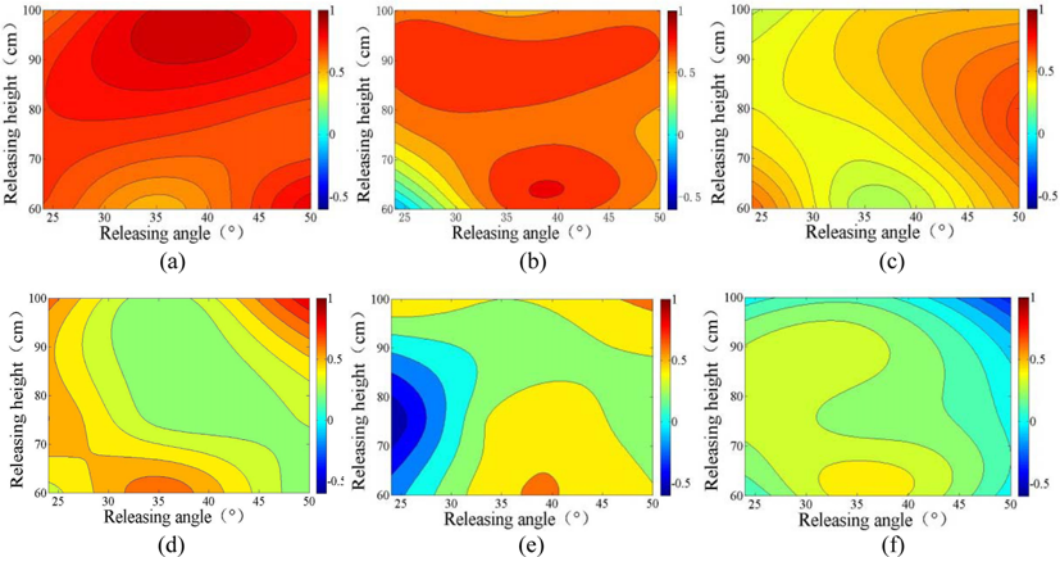

Fig. 10. Effect of Slope Angle and Block Shape on the Energy Loss Rate: (a) Plate with Slope Angle 15°, (b) Plate with Slope Angle 20°, (c) Plate with Slope Angle 30°, (d) Strip with Slope Angle 15°, (e) Strip with Slope Angle 20°, (f) Strip with Slope Angle 30°

angle, which agrees with the observations of Wu (1985) and Chau (2002). For the plate blocks, the maximum value of COR appears near releasing angle 35° and 65 cm height, decreasing to the periphery. In addition, no matter what the slope angle is, the extreme value much approached to the position at releasing angle 35° and 65 cm height, which means a smaller COR. The value of COR of the strip blocks is greater than the plate blocks at the same slope angle.

Figure 10 plots the relationship between the kinetic energy loss rate and slope angle. In comparison with COR, the kinetic energy loss rate presented a gradually decreasing trend and when the slope angle is close to zero, a vertical collision happens with more kinetic energy loss. For the plate blocks, the kinetic energy loss rate decreased with the slope angle and a similar variation trend occurs on the strip blocks, losing sight of the range in slope angle 20°. The kinetic energy loss rate of the plate blocks is greater than that of the strip blocks, which can be verified by the variation of resultant velocities shown in Fig. 9.

4.3 Effect of Releasing Angle and Block Shape

In order to address the effect of releasing angle and the shape of blocks on the COR values, the present experiment program was performed consisting of three releasing angles, representing three typical instability models: 24° is used to simulate slope slip, 35° is used to simulate rotary instability model and 50° is used to simulate vertical falling. Fig. 11 shows the COR value versus

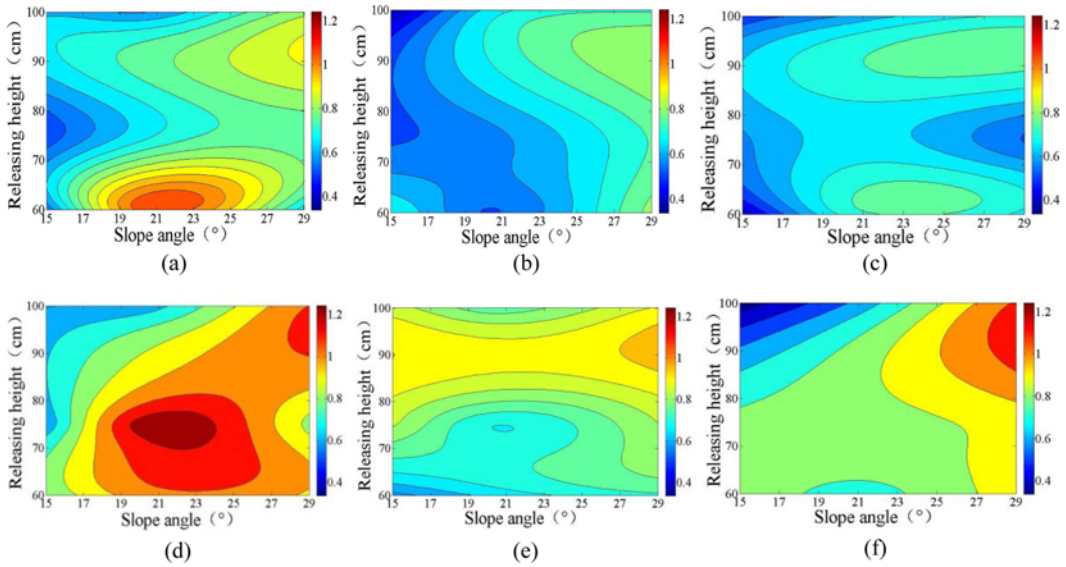

Fig. 11. Effect of Releasing Angle and Block Shape on the COR: (a) Plate with Releasing Angle 24°, (b) Plate with Releasing Angle 35° (c) Plate with Releasing Angle 50°, (d) Strip with Releasing Angle 24°, (e) Strip with Releasing Angle 35°, (f) Strip with Releasing Angle 50°

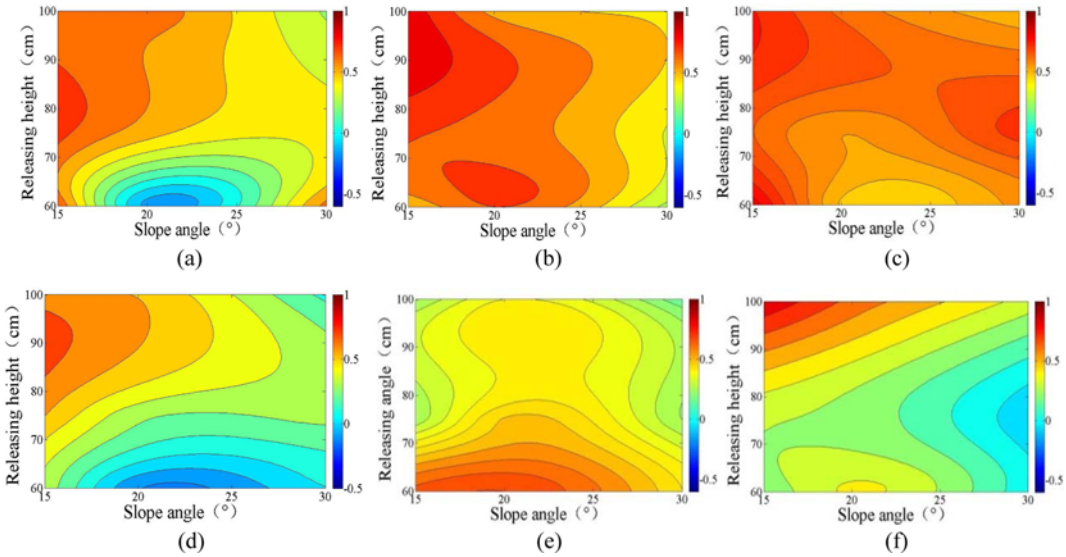

Fig. 12. Effect of Releasing Angle and Block Shape on the Kinetic Energy Loss Rate: (a) Plate with Releasing Angle 24°, (b) Plate with Releasing Angle 35° (c) Plate with Releasing Angle 50°, (d) Strip with Releasing Angle 24°, (e) Strip with Releasing Angle 35°, (f) Strip with Releasing Angle 50°

releasing angle and the shape of block. For the plate blocks, the maximum value of COR is obtained near the slope angle 22° and the releasing height 60 cm with a releasing angle 24°. Furthermore, for the plate and strip block, the coefficient of restitution initially decreases with increasing releasing angle and then increases with an increase in the releasing angle slightly. It also can be concluded that the value of COR of the strip block is greater than that of the plate under the same releasing angle.

For both shapes of blocks, the value of kinetic energy loss rate with releasing angle of 35° and 50° is close, rather greater than that with the releasing angle of 24°. However, the kinetic energy loss rate of the plate block is greater than that of the strip. Especially for the strip block, the minimum value is considerably small, near slope angle 22° and 60 cm height.

4.4 Effect of the Impacting Angle

Based on the results of falling blocks testing, the relation between the impacting angle and reflection angle of the collision is shown in Fig. 13. In the case of perfectly elastic collision, the energy before and after the collision are identical. Therefore, ideally, all the points should be in the line with an angle of 45° presented in Fig. 13. However, it can be observed that all the points are below the line showing kinetic energy after the collision is less than that before the collision, which agrees with

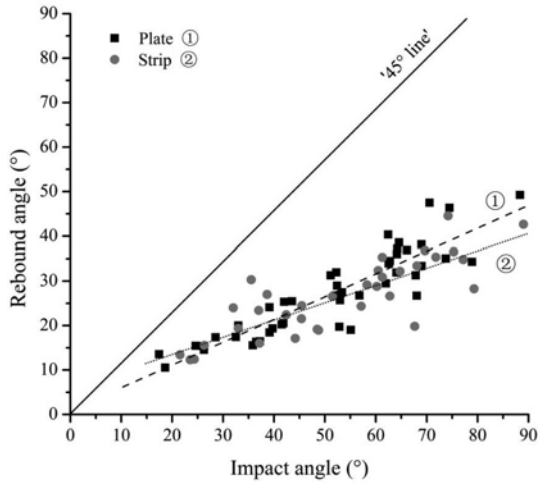

Fig. 13. Rebound Angle Versus Impact Angle for Plate and Strip Blocks

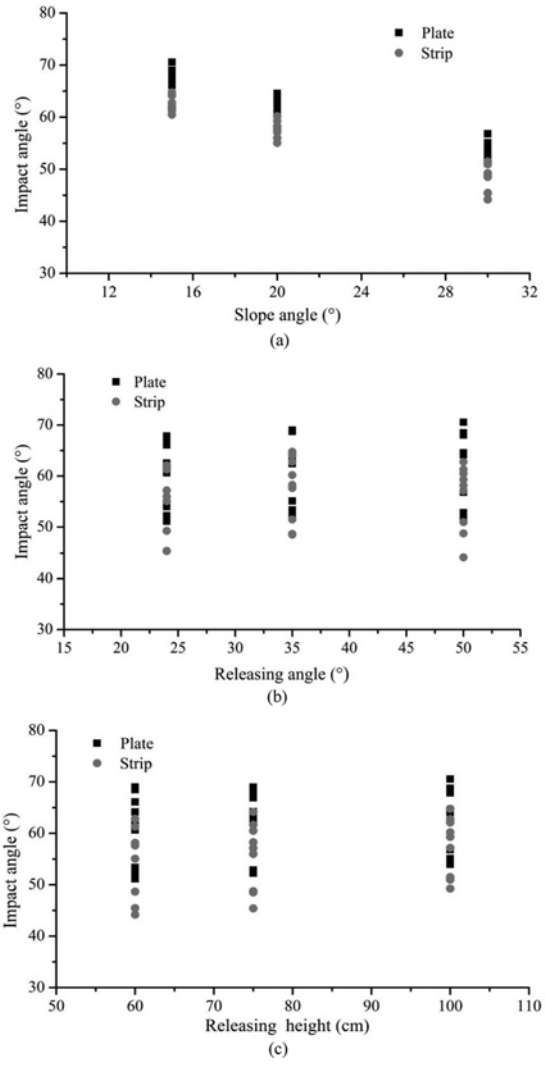

Fig. 14. Impact Angle Versus Slope Angle, Releasing Angle and Height: (a) Impact Angle Versus Slope Angle, (b) Impact Angle Versus Slope Angle, (c) Impact Angle Versus Releasing Height

the observation given by P. Asteriou (2002). In practice, energy loss always happens in collision and Fig. 13 shows a positive correlation between rebound angle and impact angle by correlation analysis and linear fitting, which is more significant in the plate blocks.

To examine the effects of slope angle, releasing angle and height on impacting angle, a series of experiments were carried out and the testing results are shown in Fig. 14. Fig. 14(a) shows the relation between impacting angle and the angle of the slope. From the distribution of the points, we can see impacting angle decreases with increasing slope angle for the same shape of blocks and the impacting angle of the strip block is smaller. However, there is no clear relation between impacting angle and the releasing angle and height, while the impacting angle of the strip blocks is a bit smaller than that of the plate blocks.

The COR values in relation to the impacting angle are presented in Fig. 15. It is observed that the COR values of the plate and strip block are higher as the impacting angle decreases. Furthermore, plate blocks obtain higher COR values compared to strip blocks. When impacting angle is equal to 90°, the slope angle is zero, which means a free falling. Two trend lines have been plotted in Fig. 15, and additionally the mean values from the same shape of blocks are presented for an impacting angle of 90°, which indicates the decreasing trend of COR with impacting angle. It should be noted that the standard deviation of two shapes of blocks is greater with increasing impacting angle,

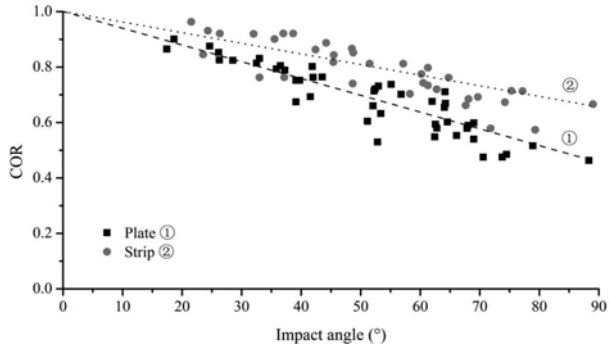

Fig. 15. Relationship between COR and Impact Angle

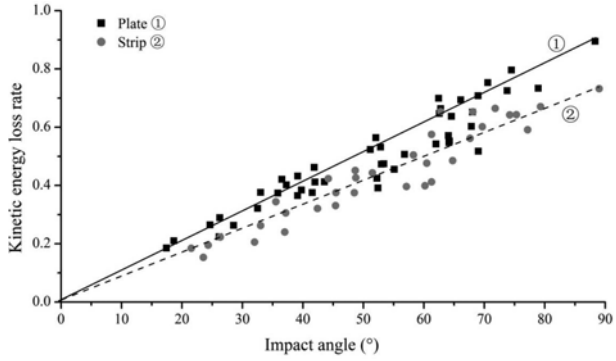

Fig. 16. Relationship between Kinetic Energy Loss Rate and Impact Angle

especially when impacting angle is higher than 45°. However, Fig. 16 shows that the rate of kinetic energy loss is higher as the impacting angle increases in contrast to normal COR trends, of which the strip is smaller compared with the plate. For plate and strip blocks, the standard deviation is greater with increasing impacting angle, similar to COR trend.

4.5 Effect of the Kinetic Energy before and after the Collision

The magnitudes of the rebounding and incoming velocities can be calculated using Eqs. (3) to (6). The kinetic energy of blocks before and after the collision can also be evaluated once the velocities and masses of blocks are obtained. The relationships between COR and kinetic energy before and after the collision are plotted in Fig. 17 and 18. Fig. 17 shows that the COR versus kinetic energy before the collision has a clear parallel arrangement trend. In addition, the strip presents a more discrete distribution and is larger than the plate. The minimum values of COR are approximately identical, and the maximum values decreases with increasing kinetic energy before the collision. However, the testing results show that there are apparent changes in the effect of kinetic energy after the collision on COR, the details of which are presented in Fig. 18. It is observed that the maximum value of COR of the plate and strip blocks are approximately identical after the collision and the distribution of plate blocks is rather discrete compared to the strip. However, a clear scattering trend from the point (0, 0.2) has been presented, which is marked by dotted lines.

For both plate and strip blocks, the kinetic energy loss rate of versus kinetic energy before and after the collision is plotted in Fig. 19 and 20 respectively. Fig. 19 shows that the points were uniform and parallel arrangement in trapezoidal area marked by dotted line before the collision. From the coefficient of restitution it can be seen that a more discrete distribution is in the strip block. Furthermore, the maximum value of kinetic energy loss rate of both blocks is close to each other. After the collision, there is an apparent change observed in the distribution characteristics, turning into scattering state with a focal point (0, 1) on the top left corner (seen Fig. 20). However, the values of loss rate mainly cluster at the range 0.2-0.8 and the kinetic energy loss rate of the plate is slightly greater than that of the strip.

In the present paper, the kinetic energy loss rate between kinetic energy before and after the collision was obtained by experiment, which can be adopted to estimate the energy of rock

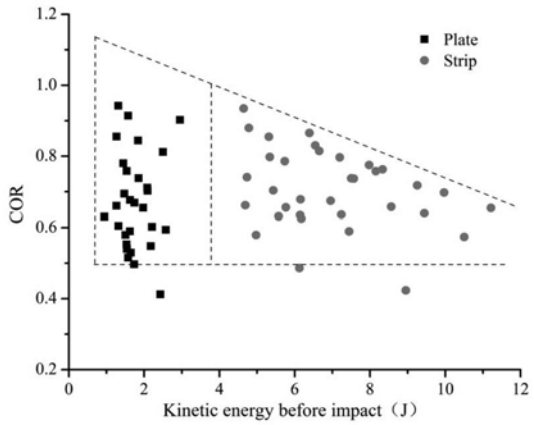

Fig. 17. Relationship between COR and Kinetic Energy before Impact

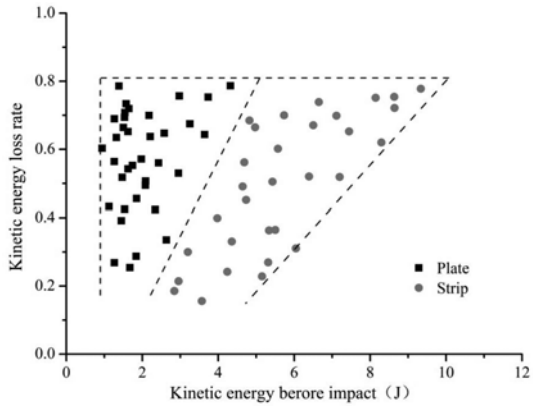

Fig. 19. Relationship between Kinetic Energy Loss Rate and Kinetic Energy before Impact

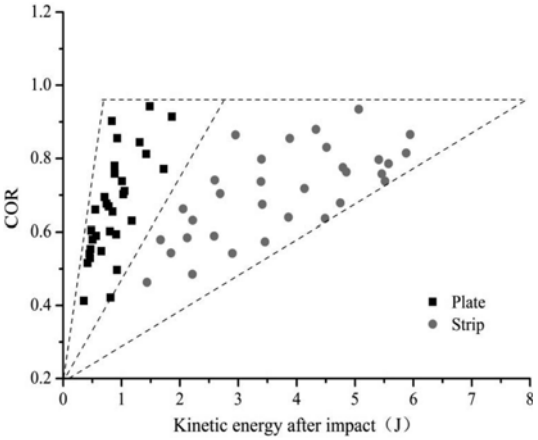

Fig. 18. Relationship between COR and Kinetic Energy after Impact

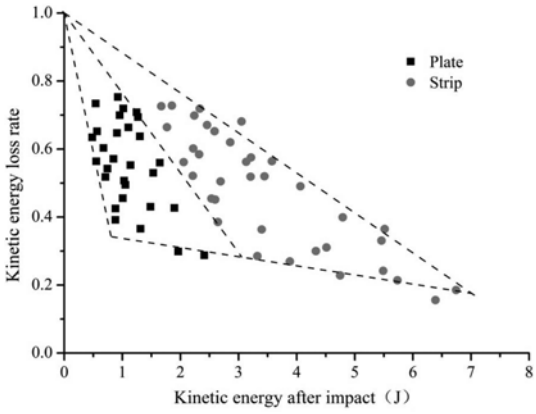

Fig. 20. Relationship between Kinetic Energy Loss Rate and Kinetic Energy after Impact

after collision. For practical purposes, this can be used to make protective measures (Gentilini *et al*., 2013; Alejano *et al*., 2007; Azzoni *et al*., 1995; Cazzani *et al*., 2005).

5. Conclusions

Since the coefficient of restitution is a key parameter to determine the travel distance, height of boulder and energy variation simulated by computer program, a reliable estimate of coefficient of restitution and kinetic energy loss rate are crucial to design remedial measures. However, there is still no agreement on which definition of COR is a better one for rockfall trajectory prediction.

In the present study, an apparatus specifically built for this study was established and two serious tests were conducted. To estimate the effect of parameters on coefficient of restitution and kinetic energy loss rate, the shape of blocks, releasing height, slope angle, releasing angle, impacting angle and kinetic energy before and after the collision were altered during the test. The results were presented through nephogram of Matlab software. It is observed that for the same kind of block, coefficient of restitution of height 75 cm is rather greater than the circumstance of 60 cm and 100 cm. Besides, the coefficient of restitution showed apparent increasing trend with the slope angle, which can be verified by the observations of Wu (1985) and Chau, K.T (2002) and the maximum value of coefficient of restitution is near slope angle 30° and releasing angle 24° respectively .On a whole, the COR of strip block is greater compared to plate blocks. For kinetic energy loss rate, the minimum value pretend to be near height 75 cm, slope angle 30° and releasing angle 24° respectively, in contrast to normal COR trends.

The collision reflection angle is less than impact angle for all, which proves to us that energy loss always happens in the process of collision. The results demonstrated that impact angle decreases with increasing slope angle. Nevertheless, there was no obvious effect of releasing height and releasing angle on impact angle. With the increasing of impact angle, the relevant coefficient of restitution decreased and contrary to this, kinetic energy loss rate increased significantly. Finally, the changing trend of COR and kinetic loss rate versus kinetic energy before and after the collision is proposed. Compared to plate blocks, a larger distribution area was formed by kinetic energy points of the strip both before and after the collision. Additionally, a parallel trapezoidal distribution of kinetic energy turned into a scattering, which can provide basis for mitigation measures.

Acknowledgements

This work was supported by the State Key Development Programfor Basic Research of China (No. 2013CB036000), the State Key Program of National Natural Science of China (No.51139004), the National Natural Science Foundation Item of China (No. 51479106), the Natural Science Foundation Item of Shandong province (No. 2014ZRE27303) and the Independent Innovation Foundation of Nanjing Hydraulic Research Institute (No. YN914005).

References

Agliardi, F. and Crosta, G. B. (2003). "High resolution three-dimensional numerical modelling of rockfalls." *International Journal of Rock Mechanics and Mining Sciences*, Vol. 40, No. 4, pp. 455-471, DOI: 10.1016/S1365-1609(03)00021-2.

Alejano, L. R., Pons, B., Bastante, F. G., Alonso, E., and Stockhausen, H. W. (2007). "Slope geometry design as a means for controlling rockfalls in quarries." *International Journal of Rock Mechanics and Mining Sciences*, Vol. 44, No. 6, pp. 903-921, DOI: 10.1016/j.ijrmms.2007.02.001.

Asteriou, P., Saroglou, H., and Tsiambaos, G. (2012). "Geotechnical and kinematic parameters affecting the coefficients of restitution for rock fall analysis." *International Journal of Rock Mechanics and Mining Sciences*, Vol 54, pp. 103-113, DOI: 10.1016/j.ijrmms.2012.05.029.

Azzoni, A. and De Freitas, M. H. (1995). "Experimentally gained parameters, decisive for rock fall analysis." *Rock Mechanics and Rock Engineering*, Vol. 28, No. 2, pp. 111-124, DOI: 10.1007/BF01020064.

Azzoni, A., La Barbera, G., and Zaninetti, A. (1995). "Analysis and prediction of rockfalls using a mathematical model." *International Journal of Rock Mechanics and Mining Sciences,* Vol. 32, No. 7, pp. 709-724, DOI: 10.1016/0148-9062(95)00018-C.

Bozzolo, D. and Pamini, R. (1986). "Simulation of rock falls down a valley side." *Acta Mech*, Vol. 63, pp. 113-130, DOI: 10.1007/BF01182543.

Buzzi, O., Giacomini, A., and Spadari, M. (2012). "Laboratory investigation on high values of restitution coefficients." *Rock Mechanics and Rock Engineering*, Vol. 45, No. 1, pp. 35-43, DOI: 10.1007/s00603-011-0183-0.

Cazzani, A., Mongiovı, L., and Frenez, T. (2002). "Dynamic finite element analysis of interceptive devices for falling rocks." *International Journal of Rock Mechanics and Mining Sciences*, Vol. 39, No. 3, pp. 303-321, DOI: 10.1016/S1365-1609(02)00037-0.

Chau, K. T., Wong, R. H. C., and Wu, J. J. (2002). "Coefficient of restitution and rotational motions of rockfall impacts." *International Journal of Rock Mechanics and Mining Sciences*, Vol. 39, No. 1, pp. 69-77, DOI: 10.1016/S1365-1609(02)00016-3.

Chau, K. T., Wong, R. H. C., Liu, J., Wu, J. J., and Lee, C. F. (1999). *Shape effects on the coefficient of restitution during rockfall impacts*, In 9th ISRM Congress., International Society for Rock Mechanics, Paris. pp. 541-544.

Descoeudres, F. and Zimmermann, T. H. (1987). *Three-dimensional dynamic calculation of rockfalls*, In 6th ISRM Congress., International Society for Rock Mechanics, Montreal.

Gentilini, C., Gottardi, G., Govoni, L., Mentani, A., and Ubertini, F. (2013). "Design of falling rock protection barriers using numerical models." *Engineering Structures*, Vol. 50, pp. 96-106, DOI: 10.1016/j.engstruct.2012.07.008.

Guzzetti, F., Crosta, G., Detti, R., and Agliardi, F. (2002). "STONE: A computer program for the three-dimensional simulation of rock-falls." *Computers & Geosciences*, Vol. 28, No. 9, pp. 1079-1093, DOI: 10.1016/S0098-3004(02) 00025-0.

Huang, R. Q., Liu, W. H., Zhou, J. P., and Pei, X. J. (2007). "Rolling tests on movement characteristics of rock blocks." *Chinese Journal of Geotechnical Engineering*, Vol. 29, No. 9, pp. 1296-1302, DOI: 10.3321/j.issn:1000-4548.2007.09.003.

Japan-Road-Association. (1983). *Rockfall Handbook*, Tokyo.

Pantelidis, L. (2009). "Rock slope stability assessment through rock mass classification systems." *International Journal of Rock Mechanics and Mining Sciences*, Vol. 46, No. 2, pp. 315-325, DOI: 10.1016/j.ijrmms.2008.06.003.

Pantelidis, L. (2010). "An alternative rock mass classification system for rock slopes." *Bulletin of engineering geology and the environment*, Vol. 69, No. 1, pp. 29-39, DOI: 10.1007/s10064-009-0241-y.

Paronuzzi, P. (1989). "Probabilistic approach for design optimization of rockfall protective barriers." *Quarterly Journal of Engineering Geology and Hydrogeology*, Vol. 22, No. 3, pp. 175-183, DOI: 10.1144/GSL.QJEG. 1989.022.03.02.

Pfeiffer, T. and Bowen, T. (1989) Computer simulation of rock falls. *Bull Assoc Eng Geol*, Vol. 26, pp. 135-146.

Spang, R. M. and Rautenstrauch, R. W. (1988). "Empirical and mathematical approaches to rockfall protection and their practical applications." In Proc. 5th Int. Symp., *Landslides*, Lausanne, pp. 1237-1243.

Spang, R. M., and Sonser, T. (1995). *Optimized rockfall protection by* '*ROCKFALL*', In 8th ISRM Congress. International Society for Rock Mechanics.

Stevens. W. (1998) "Rocfall: A tool for probabilistic analysis, design of remedial measures and prediction of rock falls." *Master's thesis, Department of Civil Engineering,* University of Toronto. Ontario.